Northwell Health℠

Journal Articles

2014

Diagnosis of abnormal biliary copper excretion by positron emission tomography with targeting of (64)Copper-asialofetuin complex in LEC rat model of Wilson's disease

R. Bahde

S. Kapoor

K. K. Bhargava
Zucker School of Medicine at Hofstra/Northwell

C. J. Palestro
Zucker School of Medicine at Hofstra/Northwell

S. Gupta

Follow this and additional works at: https://academicworks.medicine.hofstra.edu/publications

 Part of the Radiology Commons

Recommended Citation

Bahde R, Kapoor S, Bhargava K, Palestro C, Gupta S. Diagnosis of abnormal biliary copper excretion by positron emission tomography with targeting of (64)Copper-asialofetuin complex in LEC rat model of Wilson's disease. . 2014 Jan 01; 4(6):Article 1936 [p.]. Available from: https://academicworks.medicine.hofstra.edu/publications/1936. Free full text article.

This Article is brought to you for free and open access by Donald and Barbara Zucker School of Medicine Academic Works. It has been accepted for inclusion in Journal Articles by an authorized administrator of Donald and Barbara Zucker School of Medicine Academic Works. For more information, please contact academicworks@hofstra.edu.

Am J Nucl Med Mol Imaging 2014;4(6):537-547
www.ajnmmi.us /ISSN:2160-8407/ajnmmi0001381

Original Article

Diagnosis of abnormal biliary copper excretion by positron emission tomography with targeting of ^{64}Copper-asialofetuin complex in LEC rat model of Wilson's disease

Ralf Bahde[1,2], Sorabh Kapoor[1], Kuldeep K Bhargava[3,4], Christopher J Palestro[3,4], Sanjeev Gupta[1]

[1]Marion Bessin Liver Research Center, Diabetes Center, Cancer Research Center, Departments of Medicine and Pathology, Ruth L. and David S. Gottesman Institute for Stem Cell and Regenerative Medicine Research, and Institute for Clinical and Translational Research, Albert Einstein College of Medicine, Bronx, NY, USA; [2]Department of Surgery, Hospital of The University of Muenster, Muenster, Germany; [3]Division of Nuclear Medicine and Molecular Imaging, North Shore-Long Island Jewish Health System, New Hyde Park, NY, USA; [4]Hofstra North Shore-LIJ School of Medicine, Hempstead, NY, USA

Received July 10, 2014; Accepted August 2, 2014; Epub September 6, 2014; Published September 15, 2014

Abstract: Identification by molecular imaging of key processes in handling of transition state metals, such as copper (Cu), will be of considerable clinical value. For instance, the ability to diagnose Wilson's disease with molecular imaging by identifying copper excretion in an ATP7B-dependent manner will be very significant. To develop highly effective diagnostic approaches, we hypothesized that targeting of radiocopper via the asialoglycoprotein receptor will be appropriate for positron emission tomography, and examined this approach in a rat model of Wilson's disease. After complexing ^{64}Cu to asialofetuin we studied handling of this complex compared with ^{64}Cu in healthy LEA rats and diseased homozygous LEC rats lacking ATP7B and exhibiting hepatic copper toxicosis. We analyzed radiotracer clearance from blood, organ uptake, and biliary excretion, including sixty minute dynamic positron emission tomography recordings. In LEA rats, ^{64}Cu-asialofetuin was better cleared from blood followed by liver uptake and greater biliary excretion than ^{64}Cu. In LEC rats, ^{64}Cu-asialofetuin activity cleared even more rapidly from blood followed by greater uptake in liver, but neither ^{64}Cu-asialofetuin nor ^{64}Cu appeared in bile. Image analysis demonstrated rapid visualization of liver after ^{64}Cu-asialofetuin administration followed by decreased liver activity in LEA rats while liver activity progressively increased in LEC rats. Image analysis resolved this difference in hepatic activity within one hour. We concluded that ^{64}Cu-asialofetuin complex was successfully targeted to the liver and radiocopper was then excreted into bile in an ATP7B-dependent manner. Therefore, hepatic targeting of radiocopper will be appropriate for improving molecular diagnosis and for developing drug/cell/gene therapies in Wilson's disease.

Keywords: ATP7B, diagnosis, metal complex, positron emission tomography, radiocopper, therapy, Wilson's disease

Introduction

In excessive amounts, transition-state metals, such as copper (Cu), pose health hazards. Metals may accumulate via increased dietary intake or abnormal handling in the body. For instance, mutations in hepatobiliary Cu transporter gene, ATP7B, cause Wilson's disease (WD) [1], leading to Cu toxicosis and liver and brain damage [2]. Early diagnosis of WD is important because Cu may be removed by drugs and cell/gene therapies [3-5]. The diagnosis of WD is generally difficult without a high index of suspicion and in fact is often missed because of its rarity (the prevalence of mutant ATP7B alleles is only 1:30,000). Percutaneous liver biopsy for Cu content measurement, the standard diagnostic procedure for WD, has the potential for serious complications. Liver Cu content measurements, the availability of which is limited in many clinical settings, may be confounded by normal or near-normal Cu levels in early WD, false negative results due to inadequate tissue sampling, or difficulty in separating homozy-

gous and heterozygous states. The alternative of genetic diagnosis in WD may be hampered by incomplete mapping of disease mutations in ATP7B gene, which currently approach approximately 500 mutations, as well as lack of reliable assays to establish the function of novel ATP7B mutations. Similarly, understanding whether Cu could be mobilized will be helpful for therapeutic development as well as monitoring treatment. Therefore, a molecular imaging technique capable of demonstrating ATP7B protein function is highly clinically relevant.

Recently, we and others determined that positron emission tomography (PET) with ^{64}Cu was appropriate for molecular imaging in WD, as in mutant rats or mice lacking ATP7B function [6, 7]. Multiple cellular mechanisms regulate hepatic Cu handling, including those involved in intracellular entry, utilization and trafficking of Cu [8]. Of these, intracellular transfer of Cu atoms to ATP7B protein and then transport of ATP7B-bound Cu to bile canaliculi constitute key physiological steps in Cu excretion with most relevance for molecular imaging in WD. Previously, in an effort to overcome issues related to the ubiquitous distribution and uptake of free ^{64}Cu with gradual release, reuptake and re-release from organs over many hours [9], we utilized ^{64}Cu-histidine [6, 10]. The Cu-histidine complex has been extensively studied over several decades [11]. Although histidine has high affinity for Cu, rapid entry and dissociation of this complex in hepatocytes led to the prompt appearance in bile of Cu in Long-Evans Agouti (LEA) rats, where ATP7B function is normal [6, 10], while in Long-Evans Cinnamon (LEC) rats, where ATP7B is non-functional, which is similar to people with WD, Cu-histidine complex was incorporated in liver but Cu did not appear in bile [6, 10]. However, as ^{64}Cu-histidine complex too was widely distributed in tissues, we considered that hepatic targeting of Cu will be superior for diagnostic applications of PET, and also for evaluating the success of liver-directed cell/gene therapy studies.

Here, we focused on receptor-mediated endocytosis, since unlike Cu uptake by Ctr1 which is expressed in cells throughout the body [8], the asialoglycoprotein receptor (ASGPR) is uniquely expressed in hepatocytes [12]. Our hypothesis was that the ^{64}Cu-AF complex should have been targeted to the liver followed by transfer in hepatocytes to ATP7B and then excretion into bile (**Figure 1**). After delivering ligands to cytoplasmic endosomes, ASGPR recycles to the hepatocyte cell membrane [13]. Consequently, ASGPR ligands were effective for hepatic targeting of nucleic acids, proteins, synthetic compounds, biomaterials, etc., including for imaging with magnetic resonance, single photon emission tomography, and other modalities [14-19]. Previously, one such ligand, asialofetuin (AF), was effective for hepatic targeting of radiotracers, and successfully identified ASGPR expression in transplanted hepatocytes that were located outside the liver [20]. In this investigation, we describe a complex of ^{64}Cu and AF, and its utilization for hepatic uptake and bile excretion studies in LEA and LEC rats.

Material and methods

Chemicals

Reagent-grade chemicals and AF were purchased from Sigma Chemical Company (St. Louis, MO).

^{64}Cu and ^{64}Cu-AF complex

We purchased ^{64}Cu chloride from MDS Nordion (Catalog IPG-Cu-64; Ottawa, Canada), with specific activity of 962 MBq/μg. We added to 50 μg AF in 500 μL 0.1 M 4-(2-hydroxyethyl)-1-piperazineethanesulfonic acid (HEPES), pH 7.4, containing 50 mM dithiothereitol, 185-200 MBq ^{64}Cu for 15 min at room temperature. The ^{64}Cu-AF complex was purified by passing through Sep-Pak C18 cartridges (WAT023501, Waters Corp., Milford, MA), which were pre-washed with 10 mL ethanol and then 10 mL water as previously described [6]. After injecting ^{64}Cu-AF, cartridges were washed with 5 mL water. We eluted ^{64}Cu-AF in 3 mL ethanol yielding 176-190 MBq activity. Specific activity of ^{64}Cu-AF was 3.52-3.80 GBq per mg. Purity and stability of ^{64}Cu-AF complex was examined by instant thin layer chromatography (ITLC) with acetone as solvent. The mobile phase was analyzed by dividing ITLC strips and measuring activity in well counter. ^{64}Cu-AF was ≥95% pure.

Animals

Animal Care and Use Committees and Radiation Safety Committees at Albert Einstein College of Medicine and Feinstein Institute of Medical Research, North Shore - Long Island Jewish Health System, approved the protocols. LEA

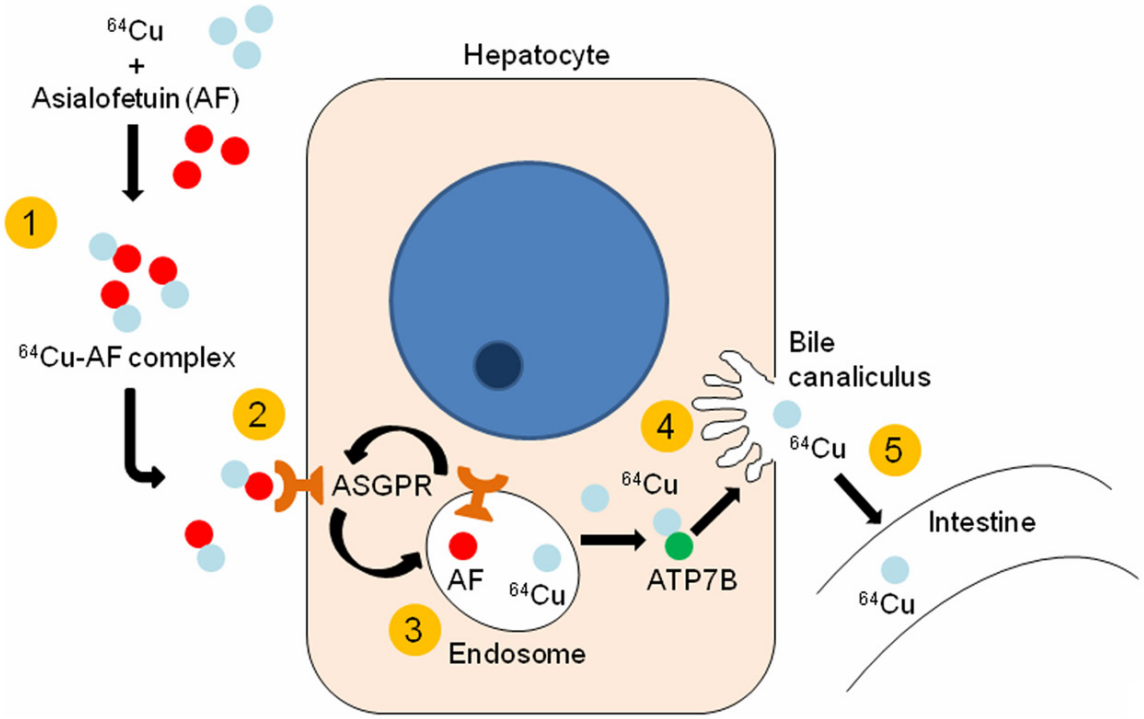

Figure 1. Schematic representation of proposed hypothesis for imaging of ATP7B function with ^{64}Cu-asialofetuin (AF). After complexing of ^{64}Cu and AF (Step 1), the complex should enter hepatocytes via asialoglycoprotein receptor (ASGPR) (Step 2). The ASGPR-bound ^{64}Cu-AF complex should be internalized in endosomes followed by dissociation from ASGPR and breakdown of the complex with separation of ^{64}Cu and AF (Step 3). ATP7B in cytoplasm should then accept ^{64}Cu (Step 4). Next, ATP7B should transport ^{64}Cu into bile canaliculi, leading to intestinal excretion (Step 5).

and LEC rats, 8 to 12 weeks old and weighing 250-300 g, were from Special Animal Core of Marion Bessin Liver Research Center. All animals were allowed pelleted food and water throughout. Animals were genotyped by polymerase chain reaction (PCR) of genomic DNA [21]. Hepatic ATP7B mRNA was shown by reverse transcription-PCR (RT-PCR) with RNA extracted by Trizol Reagent. Primers were: ATP7B: 5'-CCATCTCCAGTGATATCAGTG-3' (forward); 5'-CGCACAGCACACCATCAATGG-3' (reverse); rat β-actin: 5'-CCCTGGCTCCTAGCACCAT-3' (forward) and 5'-AGAGCCACCAATCCACACAGA-3' (reverse). Only wild-type healthy LEA rats and LEC rats homozygous for ATP7B mutation were used for studies.

We divided 12 LEA rats and 12 LEC rats into groups of 3-4 rats each. Rats were anesthetized with ketamine and xylazine (Fort Dodge Animal Health, Fort Dodge, Iowa) for all studies. For imaging, anesthesia was continued with inhaled isoflurane. Bile was cannulated with a catheter by midline laparotomy, as previously described [6], and then 3.7-5.5 MBq ^{64}Cu-AF was injected intrasplenically under direct vision. We had validated in previous studies that intrasplenic injection produces results similar to to those obtained with tail vein injection [6]. Previous studies established that neither bile cannulation nor bile collection altered excretion of ^{64}Cu or ^{64}Cu-histidine complex.

Protocols for hepatic handling of ^{64}Cu

For blood clearance of ^{64}Cu-AF, we obtained samples from tail-cut every 15 min for 1 h. Bile was collected at 15 min intervals between 0-1 h after injection of ^{64}Cu-AF. Bile flow rates were 1.8 ± 0.4 ml per hour. Liver, kidneys, spleen, heart and lung samples were collected at sacrifice of animals. Total weights of organs were measured. Tissue radioactivity was measured simultaneously with decay correction. Organ activity was normalized against heart muscle for background, which was taken as zero activity, and then expressed on per gram basis followed by conversion to total organ weights, as previously described [6]. To correlate loss of hepatic ^{64}Cu after 1 h in microPET images we divided bile counts by liver plus bile counts.

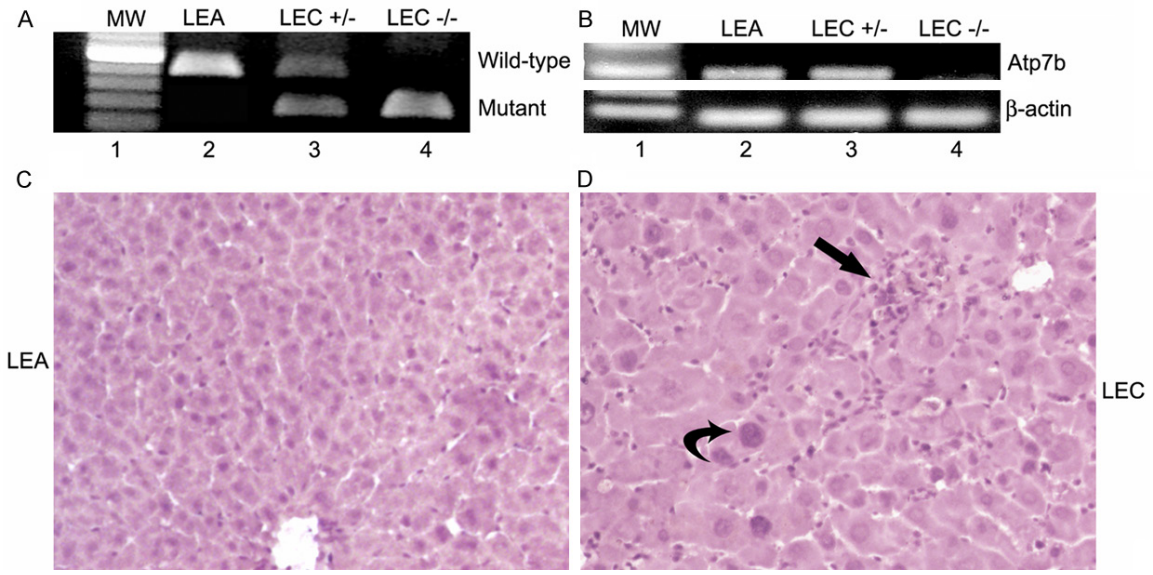

Figure 2. Characterization of animals. A. DNA PCR showing correct genotype of Atp7b alleles in healthy LEA rats (single band of wild-type allele), heterozygous LEC+/- rats (bands for both wild-type and mutant alleles) and homozygous LEC-/- rats (single band of mutant allele). B. Shows no Atp7b mRNA in LEC-/- rats. C. Normal liver histology in LEA rat. D. LEC rat with liver abnormalities, including bile duct proliferation, inflammatory cell infiltrates (straight arrow) and megalonuclei (curved arrow).

For microPET, animals were spread supine and imaging was centered on the upper abdomen. Image acquisitions began with 350-650 keV windows before injection of activity (R4 Scanner, Concorde MicroSystems, Knoxville, TN). Sixty min dynamic PET recording was performed with 2 min frames. Image analysis incorporated isotope decay, scatter, dead-time and arc corrections by ASIPro software (Siemens Medical Solutions USA, Inc., Knoxville, TN). Hepatic regions of interest in equal volumes were selected away from liver edge and diaphragm to decrease respiratory artifacts. Standardized uptake values (SUV) were plotted against time and time-to-peak hepatic SUV (T-SUVmax) was determined with linear regression for differences in ^{64}Cu activity as previously established [6].

Histological analysis

Cryostat sections of 5 μm thickness were prepared from tissues frozen in methylbutane at -80°C. Acetone-fixed sections were stained with hematoxylin and eosin.

Statistical analysis

Data are expressed as means ± SEM. Analyses used t-tests or ANOVA with SigmaStat (Systat Inc., Point Richmond, California, USA). *P* values <0.05 were considered significant.

Results

Genotyping

DNA PCR confirmed the presence of healthy ATP7B gene copies in LEA rats and ATP7B homozygous mutant alleles in LEC rats (**Figure 2A**). ATP7B mRNA was present in LEA rats, but not in LEC rats (**Figure 2B**). Liver morphology was normal in LEA rats, while in LEC rats, changes characteristic of Cu toxicosis including enlarged hepatocytes containing megalonuclei, bile duct proliferation and cholangiofibrosis, were present [4-6].

Blood clearance

After injection of ^{64}Cu in LEA rats (n=3), activity cleared gradually from the blood, Of the total blood activity present at 15 min (100%), 90 ± 5%, 78 ± 3% and 76 ± 6% remained at 30, 45 and 60 min, respectively (**Figure 3**). ^{64}Cu-AF cleared significantly more rapidly ($p<0.05$) in LEA rats (n=3), with 78 ± 0.5%, 66 ± 2% and 57 ± 2% of the total blood activity at 15 min remaining at 30, 45 and 60 min, respectively. Twenty-five percent more activity was cleared at 1-hour in LEA rats receiving ^{64}Cu-AF than in animals receiving ^{64}Cu.

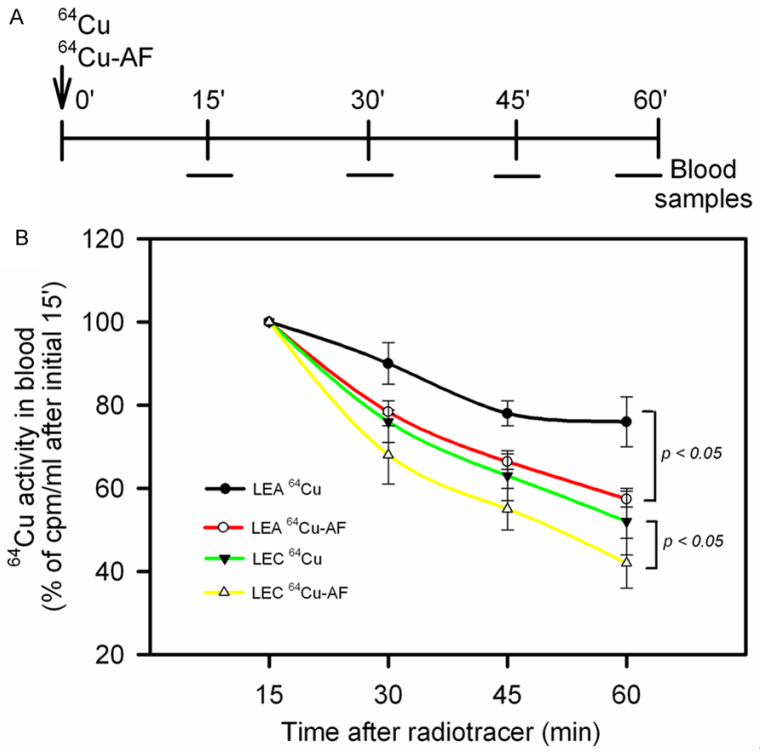

Figure 3. Radiotracer clearance from blood. A. Study design indicating serial measurements were made 15, 30, 45 and 60 min after injection of ^{64}Cu or ^{64}Cu-AF into LEA and LEC rats (n=3 each). B. Clearance of ^{64}Cu-AF from blood was greater than that of ^{64}Cu in both LEA and LEC rats. Blood ^{64}Cu clearance was greater in LEC rats.

^{64}Cu was cleared more rapidly from the blood in LEC rats (n=3) than in LEA rats (n=3). Of total blood activity present at 15 min (100%), 76 ± 5%, 63 ± 6% and 52 ± 8%, remained at 30, 45 and 60 min, significantly less than in LEA rats ($p<0.05$, ANOVA). As with LEA rats, ^{64}Cu-AF was cleared from blood significantly more rapidly than ^{64}Cu, with 68 ± 7%, 55 ± 5% and 42 ± 6% of total blood activity present at 15 minutes, remaining at 30, 45 and 60 min, respectively ($p<0.05$, ANOVA). The difference in clearance of ^{64}Cu-AF and ^{64}Cu at 1-hour in LEC rats was 65% ($p<0.05$, ANOVA).

Organ distribution

We sampled excised organs 1-hour after radiotracer injection. In LEA rats (n=3), injected with ^{64}Cu, most of the activity was in the liver, with less activity in the kidneys and spleen, and minimal activity in the lungs (**Figure 4**). Of the total activity in these four organs 82% was in the liver, 15% was in the kidneys, 3% was in the spleen and 1.6% was in the lungs. In contrast, after injection of ^{64}Cu-AF, liver activity decreased, and renal and splenic activity increased ($p<0.05$, ANOVA). Lung activity was unchanged. Of the total activity in these four organs, 74% was in the liver, 18% in the kidneys, 5% in the spleen and 1.8% in the lungs.

In LEC rats injected with ^{64}Cu (n=3), there was significantly more activity in the liver (2.2 ± 0.4), kidneys,(3.2 ± 0.3), and spleen (3.3 ± 0.4) ($p< 0.05$, ANOVA) than in LEA rats. Lung activity (0.7%) again was negligible. When ^{64}Cu-AF was injected liver and spleen activity was even higher, 2.7 ± 0.4 and 5 ± 1.3 times greater, respectively, than in LEA rats ($p<0.05$, ANOVA). Renal activity after ^{64}Cu-AF injection was similar to that after ^{64}Cu, 2.4 ± 0.8-fold more than in LEA rats. Lung activity again was negligible. Of the total activity in these four organs, 82% was in the liver, 12% was in the kidneys, 6% was in the spleen and 0.4% was in the lungs.

Biliary excretion

Activity appeared in the bile of LEA rats within minutes after injection of both ^{64}Cu and ^{64}Cu-AF (not shown). ITLC of bile samples confirmed presence of ^{64}Cu in both groups indicating intracellular dissociation of the ^{64}Cu-AF complex. In LEA rats (n=3), 1-hour after ^{64}Cu injection, the fraction of bile activity constituted 10.0 ± 1.5% of liver plus bile activity (**Figure 5**). In LEA rats (n=3) injected with ^{64}Cu-AF the fraction of bile activity was 19.2 ± 1.0% ($p<0.05$, t-test). In LEC rats, there was no detectable bile activity after injection of ^{64}Cu or ^{64}Cu-AF (n=3 each).

MicroPET analysis of ATP7B-dependent ^{64}Cu excretion

Dynamic imaging after ^{64}Cu-AF injection in LEC and LEA rats (n=3 each) was performed to

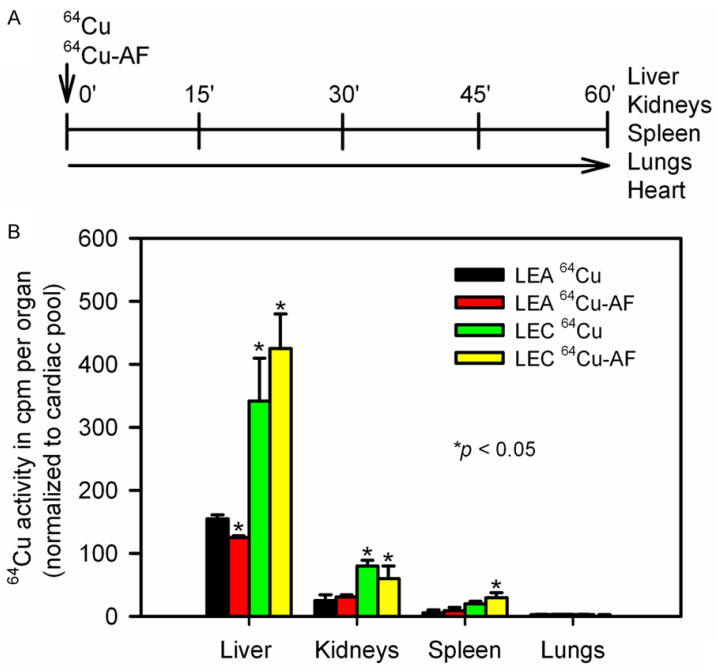

Figure 4. Incorporation of ^{64}Cu-AF in organs. A. Study design indicating organ distribution of activity was analyzed 1 hour after injection of ^{64}Cu or ^{64}Cu-AF into LEA and LEC rats (n=3 each). B. Chart shows activity in cpm x 10^4 per organ. More activity accumulated in the liver of LEC rats compared with LEA rats, which reflected continued uptake of radiotracers in the liver in the likely absence of biliary excretion. Moreover, liver activity in LEC rats was even higher after ^{64}Cu-AF, which confirmed superior hepatic targeting. By contrast, liver activity decreased more in LEA rats, suggesting greater clearance through biliary excretion. Asterisks indicate p<0.05 versus controls.

determine changes in hepatic activity over time (**Figure 6**). In LEA rats, hepatic activity increased rapidly and peaked within 5 min (T-SUVmax), decreasing by 39% at 1-hour. In contrast, hepatic activity increased in the livers of LEC rats throughout the 1-hour period. At one hour, there was nearly twice as much activity in the livers of LEC rats compared to the livers of LEA rats (p<0.05, t-test).

Discussion

These results indicate that the ^{64}Cu-AF complex was successfully targeted to hepatocytes followed by intracellular dissociation of the complex and then excretion of thus freed up radiocopper into bile. We injected radiotracers intrasplenically under direct vision to ensure their delivery. Previously, we verified that peripheral intravenous or intrasplenic injection of radiotracers produced similar distributions in the body [6, 22], although those studies did not include AF complexes. To our knowledge, studies directly comparing the distribution of AF complexes after injection into a peripheral vein or intrasplenically have not been published. However, in one previous study, injection of radiolabeled AF complexes into the tail vein of rats [23] resulted in hepatic accumulation of 100% activity over approximately 5 minutes, which was similar to our results after intrasplenic injection of ^{64}Cu-AF in healthy rats, as further discussed below.

The faster clearance from blood, more rapid uptake in liver, and greater activity in bile of healthy LEA rats given ^{64}Cu-AF versus ^{64}Cu indicated that the complex delivered greater amounts of ^{64}Cu to hepatocytes. The appearance of activity in bile was in agreement with the proposed intracellular processing of the ^{64}Cu-AF complex, leading to breakdown of the complex, transfer of dissociated ^{64}Cu to ATP7B protein, and then excretion in bile of LEA rats (**Figure 1**). By contrast, while ^{64}Cu-AF entered the liver in LEC rats, ^{64}Cu did not appear in bile, which confirms that ATP7B was required for excreting ^{64}Cu dissociated from ^{64}Cu-AF complex. These findings should fulfil requirements for diagnosing presence of ATP7B function in healthy and WD states. As humans with WD share an inability to excrete Cu in bile, the principle of using targetable Cu complexes should be suitable for molecular imaging to demonstrate presence or absence of ATP7B function in people. As biliary ^{64}Cu excretion in heterozygous LEC rats was similar to healthy LEA rats [6], molecular imaging should be helpful for separating healthy individuals and heterozygous carriers of WD alleles from those with WD and absence of ATP7B function. This fulfills an important clinical need, i.e., the recognition of healthy and diseased members in kindreds with newly diagnosed index cases of WD. It is noteworthy that liver injury or inflammation did not affect ATP7B function [6], therefore, it will be possible to distinguish between normal and abnormal Cu transport function of ATP7B from people with

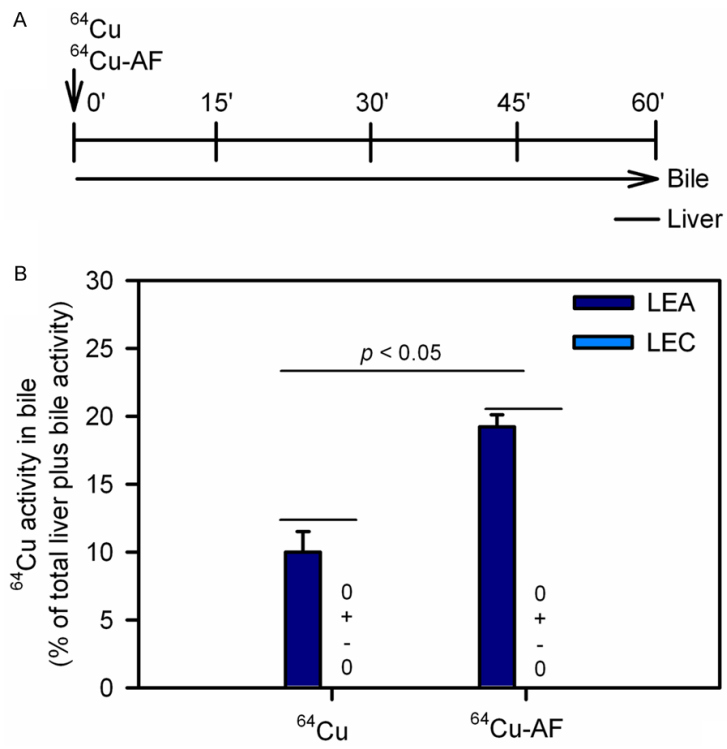

Figure 5. Biliary excretion of ^{64}Cu. A. Schematic indicating bile was collected for 60 min starting immediately before injection of ^{64}Cu or ^{64}Cu-AF into LEA and LEC rats (n=3 each). Liver was weighed and sampled for activity after 1 hour. B. Chart showing activity was excreted in bile of LEA rats but not of LEC rats. In LEA rats 10±1.5% of liver plus bile activity was in bile after ^{64}Cu, whereas 19.2±1% activity was in bile after ^{64}Cu-AF, $p<0.05$. This indicated superior hepatic targeting of ^{64}Cu-AF, as well as dissociation of the complex in hepatocytes, and transfer of ^{64}Cu ions to Atp7b for biliary excretion.

other, nonwilsonian types of acute or chronic liver diseases, which also is clinically relevant.

In hepatocytes, ATP7B is expressed, but ATP7A, which transports Cu into blood, is not [8]. In cells expressing ATP7A, which includes virtually all tissues with the exception of the kidneys where both ATP7A and ATP7B are expressed, exchanges of Cu between intracellular and extracellular pools after entry into cells via Ctr1, inevitably lead to complex kinetics of Cu reutilization. However, since Cu is excreted out of the body only by hepatic ATP7B, diagnostic applications by the proposed approach of molecular imaging in WD will not be affected by these processes, as was the case in our animal studies. This should again be the case so far as development is concerned of drugs and cell or gene therapy aimed at increasing Cu excretion in bile [6].

The biology of ASGPR-mediated endocytosis has long been studied because of its considerable physiological and pathophysiological significance [12]. In particular, the abundant cell surface expression of ASGPR is characteristic of hepatocytes, and this receptor is not displayed on any other cell type of the body. Consequently, ASGPR came to the attention of investigators for hepatic targeting. Multiple natural and synthetic ASGPR ligands have now been reported for targeting DNA, RNA, drugs, vectors, biomaterials, and imaging agents, to liver [14-19]. The latter include tagged synthetic compounds, proteins and other molecules or particles for PET, single photon emission computed tomography and magnetic resonance [14, 15, 19]. The specific advantages of ASGPR include highly efficient hepatic uptake of ASGPR ligands, e.g., in a rat study, 63% of the intravenous dose of radioiodinated asialoorosomucoid was in the liver at 10 minutes [13]. The ASGPR-bound ligands are rapidly internalized from cell surface to acidic endosomes in cytoplasm [24], where ASGPR dissociates from ligands, and returns to the cell membrane to resume receptor functions. Intracellularly-delivered ASGPR ligands, however, continue separately along their independent fates. In this way, intracellular delivery of ^{64}Cu-AF by ASGPR was more efficient, and should have led to dissociation first of ^{64}Cu-AF from ASGPR and second of ^{64}Cu from AF due to proteolytic and hydrolytic processes that are typical of acidic endosomes, before ^{64}Cu would have been transferred to ATP7B in LEA rats and not in LEC rats (**Figure 1**).

The coordination of ^{64}Cu with histidine residues may have occurred in the ^{64}Cu-AF complex, since histidine is a very strong metal coordinating ligand, probably with at least three metal-binding sites, and this property of histidine has been highly characterized [11]. Under physio-

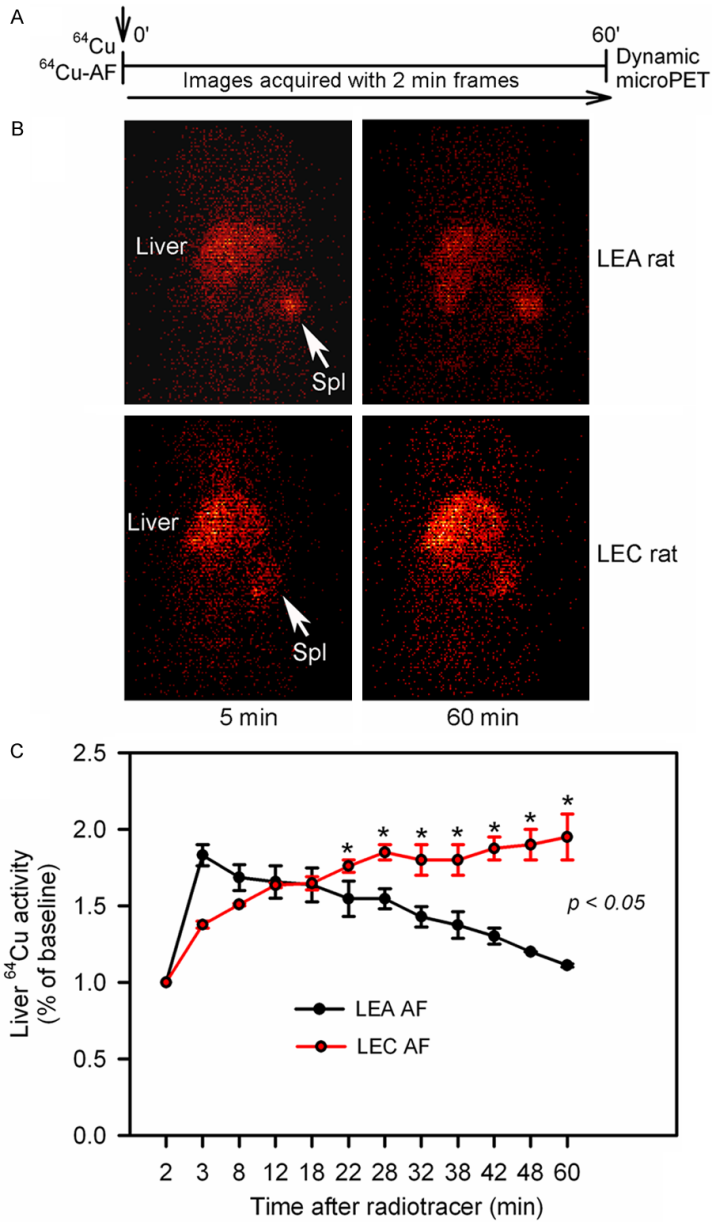

Figure 6. MicroPET for hepatic ^{64}Cu activity. A. Protocol indicating dynamic imaging was done for 60 min after injection of ^{64}Cu-AF into LEA and LEC rats (n=3 each). B. Representative sequential PET images at early and late times from LEA and LEC rats after ^{64}Cu-AF was injected into spleen (arrows, Spl). Note activity was in only liver and not kidneys, which are outlined after injection of ^{64}Cu (not shown). Moreover, more activity accumulated in liver of LEC rats from start to end. C. Hepatic SUV generated by linear regression over 1 hour after ^{64}Cu-AF. In LEA rats, activity rapidly peaked, which indicated early hepatic uptake of ^{64}Cu-AF, and decreased subsequently. In LEC rats, hepatic activity increased continually in agreement with the lack of biliary ^{64}Cu excretion. Asterisks indicate p<0.05.

logical conditions, histidine-bound Cu may exist in (2+) state with two histidine species [11], although this state may change under freezing conditions, where Cu^{2+} with four histidine species has been found [25]. Alternatively, histidine-bound Cu may also exist in (1+) state [26]. Recently, x-ray structure of Cu-histidine crystals showed coordination by two histidine species [27]. As buffers, e.g., HEPES in our studies, do not complex Cu to any significant degree [28], the potential of this buffer causing interference in studies can be confidently excluded. Of note, coordination of Cu by histidine is quite potent, such that Cu may be selectively enriched from complex mixtures by histidine columns, and histidine-bound Cu is not readily transferred to circulating proteins, e.g., albumin, which may otherwise enhance cellular Cu uptake [29]. By contrast, free Cu binds to albumin with high affinity, which interferes with its cellular uptake [30]. These advantages of histidine-Cu complex were beneficial in the treatment of people with Menkes' disease, which is due to ATP7A mutations with severe Cu deficiency [11] and proved useful for diagnostic PET in WD [6]. Nevertheless, we should emphasize that the structure of ^{64}Cu-AF complex is unknown, and requires further investigation.

More rapid clearance of blood activity after ^{64}Cu-AF compared with that of ^{64}Cu, along with hepatic uptake in LEA, as well as in LEC rats, is in agreement with the entry of this complex in an exchangeable Cu pool. More ^{64}Cu-AF cleared from blood in LEC rats. Image analysis of LEA rats receiving ^{64}Cu-AF showed that the TSUVMax of less than five minutes was shorter than that of 13 ± 2 minutes after ^{64}Cu-histidine in our previous study [6]. The blood clearance of ^{64}Cu-AF complex was greater in LEC rats, which was similar to better clearance in LEC rats of ^{64}Cu instilled into stomach [31], and also of intravenously administered ^{64}Cu-histidine complex [6]. In the case of ^{64}Cu, this was likely in agreement with the possibility of greater Cu uptake capacity in LEC rats, perhaps

as an adaptive mechanism to deal with persistently high Cu levels in blood. In the case of ^{64}Cu-AF, image analysis showed more gradual accumulation of activity in the liver of LEC rats compared with LEA rats (see **Figure 6**), which might have reflected differences in ASGPR expression levels in these animals. For instance, ASGPR expression level can decrease in response to inflammatory cytokines or liver injury, as noted during onset of fatty liver disease or alcoholic liver disease [32, 33]. However, it should be noted that for molecular imaging with this proposed approach, only trace amounts of ^{64}Cu-AF are required, which should need very little ASGPR for binding and internalization in hepatocytes. This was substantiated by necessary hepatic incorporation of ^{64}Cu-AF for successful imaging in LEC rats despite the presence of significant Cu toxicosis and liver injury.

Subsequently, biliary excretion of ^{64}Cu in ATP7B-dependent manner, i.e., in LEA rats, but not in LEC rats, indicated that the ^{64}Cu-AF complex was broken down in hepatocytes and ^{64}Cu was indeed available for transfer to ATP7B in LEA rats. Since bile ^{64}Cu excretion after ^{64}Cu-AF was significantly greater than that after ^{64}Cu alone, we surmise that this complex improves discriminant value of the molecular imaging test for the diagnosis of WD in LEC rats. Therefore, use of the hepatic SUVmax parameter with image analysis over 30-60 min after ^{64}Cu-AF will be useful for distinguishing between WD and healthy states. Previously, the specificity of ^{64}Cu-histidine complex for imaging in WD was verified by reconstitution of the molecular defect in LEC rats after liver repopulation with healthy LEA rat hepatocytes [6]. It should be noted that, based on dosimetric estimates in prior studies, administration of ^{64}Cu-AF for PET is feasible in people [7]. Such a diagnostic test will be helpful for therapeutic development in WD, including for cell and gene therapy applications, as discussed elsewhere [34].

Conclusions

We studied a ^{64}Cu-AF complex for molecular imaging of ATP7B-dependent biliary Cu excretion. Compared with ^{64}Cu, the ^{64}Cu-AF complex was more efficiently cleared from blood and was incorporated in the liver in both healthy and mutant rats lacking ATP7B function, which is characteristic of WD. This hepatic targeting of ^{64}Cu-AF complex resulted in greater excretion of activity in the bile of healthy rats compared with that of ^{64}Cu alone. In contrast, no activity was present in the bile of mutant rats deficient in ATP7B function after injection of either ^{64}Cu or ^{64}Cu-AF. This indicates that after hepatic targeting, the ^{64}Cu-AF complex broke down in hepatocytes with transfer of ^{64}Cu to ATP7B, and biliary excretion in ATP7B-dependent manner. Therefore, hepatic targeting of ^{64}Cu-AF complex was successful for molecular imaging of ATP7B function in healthy and WD states. This will offer opportunities for further diagnostic and therapeutic developments in WD.

Acknowledgements

Supported in part by NIH grants, R01 DK0-88561, R01 DK071111, P30 DK41296, P30 CA013330, and DFG grant BA 3609/1-1, Germany (RB). MicroPET was performed with E. Fine, MD, and W. Koba in Donald M. Blaufox Laboratory, Albert Einstein College of Medicine. Published in part as abstracts: Bhargava KK, et al. J Nucl Med 2012; 53 (suppl 1): (P) 338; and Bahde R, et al. Hepatology 2012; 56: 826A.

Disclosure of conflict of interest

None.

Address correspondence to: Dr. Sanjeev Gupta, Albert Einstein College of Medicine, Ullmann Building, Room 625, 1300 Morris Park Avenue, Bronx, NY 10461, USA. Tel: 718-430-3309; Fax: 718-430-8975; E-mail: sanjeev.gupta@einstein.yu.edu

References

[1] Bull PC, Thomas GR, Rommens JM, Forbes JR, Cox DW. The Wilson disease gene is a putative copper transporting P-type ATPase similar to the Menkes gene. Nat Genet 1993; 5: 327-37.

[2] Ala A, Walker AP, Ashkan K, Dooley JS, Schilsky ML. Wilson's disease. Lancet 2007; 369: 397-408.

[3] Irani AN, Malhi H, Slehria S, Gorla GR, Volenberg I, Schilsky ML, Gupta S. Correction of liver disease following transplantation of normal hepatocytes in LEC rats modeling Wilson's disease. Mol Ther 2001; 3: 302-309.

[4] Malhi H, Joseph B, Schilsky ML, Gupta S. Mechanisms to repopulate liver with healthy donor cells for phenotypic correction in the LEC rat model of Wilson disease. Regen Med 2008; 2: 165-173.

[5] Joseph B, Kapoor S, Schilsky ML, Gupta S. Bile salt-induced pro-oxidant liver damage promotes transplanted cell proliferation for correcting Wilson disease in the Long-Evans Cinnamon rat model. Hepatology 2009; 49: 1616-24.
[6] Bahde R, Kapoor S, Bhargava KK, Schilsky ML, Palestro CJ, Gupta S. Positron emission tomography with copper-64-histidine for nonivasive diagnosis of biliary copper excretion in LEC rat model of Wilson's disease. J Nucl Med 2012; 53: 961-8
[7] Peng F, Lutsenko S, Sun X, Muzik O. Positron emission tomography of copper metabolism in the Atp7b (-/-) knock-out mouse model of Wilson's disease. Mol Imaging Biol 2012; 14: 70-8.
[8] Kim BE, Nevitt T, Thiele DJ. Mechanisms for copper acquisition, distribution and regulation. Nat Chem Biol 2008; 4: 176-85.
[9] Dunn MA, Green MH, Leach RM Jr. Kinetics of copper metabolism in rats: a compartmental model. Am J Physiol 1991; 261: E115-125.
[10] Schilsky ML, Irani AN, Gorla GR, Volenberg I, Gupta S. Biliary copper excretion capacity in intact animals: correlation between ATP7B gene function, hepatic mass and copper excretion. J Biochem Mol Toxicol 2000; 14: 210-214.
[11] Deschamps P, Kulkarni PP, Gautam-Basak M, Sarkar B. The saga of copper(II)-L-histidine. Coordination Chem Rev 2005; 249: 895-909.
[12] Stockert RJ. The asialoglycoprotein receptor: relationships between structure, function, and expression. Physiol Rev 1995; 75: 591-609.
[13] Yang DY, Ouyang CH, Lu FG, Liu XW, Huang LQ. Targeting specificity and pharmacokinetics of asialoorosomucoid, a specific ligand for asialglycoprotein receptor on hepatocyte. J Dig Dis 2007; 8: 89-95.
[14] Yang W, Mou T, Peng C, Wu Z, Zhang X, Li F, Ma Y. Fluorine-18 labeled galactosyl-neoglycoalbumin for imaging the hepatic asialoglycoprotein receptor. Bioorg Med Chem 2009; 17: 7510-6.
[15] Yang W, Mou T, Shao G, Wang F, Zhang X, Liu B. Copolymer-based hepatocyte asialoglycoprotein receptor targeting agent for SPECT. J Nucl Med 2011; 52: 978-85
[16] McMahon A, O'Neill MJ, Gomez E, Donohue R, Forde D, Darcy R, O'Driscoll CM. Targeted gene delivery to hepatocytes with galactosylated amphiphilic cyclodextrins. J Pharm Pharmacol 2012; 64: 1063-73.
[17] Ma J, Huang C, Yao X, Shi C, Sun L, Yuan L, Lei P, Zhu H, Liu H, Wu X, Ning Q, Zhou C, Shen G. Inhibition of hepatitis B virus and induction of hepatoma cell apoptosis by ASGPR-directed delivery of shRNAs. PLoS One 2012; 7: e46096.
[18] Zhong Y, Yang W, Sun H, Cheng R, Meng F, Deng C, Zhong Z. Ligand-directed reduction-sensitive shell-sheddable biodegradable micelles actively deliver Doxorubicin into the nuclei of target cancer cells. Biomacromolecules 2013; 14: 3723-30.
[19] Ketkar-Atre A, Struys T, Dresselaers T, Hodenius M, Mannaerts I, Ni Y, Lambrichts I, Van Grunsven LA, De Cuyper M, Himmelreich U. In vivo hepatocyte MR imaging using lactose functionalized magnetoliposomes. Biomaterials 2014; 35: 1015-24.
[20] Nagata H, Nishitai R, Shirota C, Zhang JL, Koch CA, Cai J, Awwad M, Schuurman HJ, Christians U, Abe M, Baranowska-Kortylewicz J, Platt JL, Fox IJ. Prolonged survival of porcine hepatocytes in cynomolgus monkeys. Gastroenterology 2007; 132: 321-9.
[21] Ahmed S, Deng J, Borjigin J. A new strain of rat for functional analysis for PINA. Brain Res Mol Brain Res 2005; 137: 63-69.
[22] Joseph B, Bhargava KK, Trunco G, Kumaran V, Palestro CJ, Gupta S. Regulation of hepatobiliary transport activity and noninvasive identification of cytokine-dependent liver inflammation. J Nucl Med 2005; 46: 146-52.
[23] Abe M, Lai J, Kortylewicz ZP, Nagata H, Fox IJ, Enke CA, Baranowska-Kortylewicz J. Radiolabeled constructs for evaluation of the asialoglycoprotein receptor status and hepatic functional reserves. Bioconjug Chem 2003; 14: 997-1006.
[24] Onizuka T, Shimizu H, Moriwaki Y, Nakano T, Kanai S, Shimada I, Takahashi H. NMR study of ligand release from asialoglycoprotein receptor under solution conditions in early endosomes. FEBS J 2012; 279: 2645-56.
[25] Basosi R, Valensin G, Gaggelli E, Froncisz W, Pasenkiewicz-Gierula M, Antholine WE, Hyde JS. Multifrequency ESR of Cu(II)-(His), (His = Histidine). 1. Immobile Phase. Inorg Chem 1986; 25: 3006-3010.
[26] Venelinov T, Arpadjan S, Karadjova I, Beattie J. Properties of the copper(II)-histidine complex obtained after dialysis of human plasma with histidine. Acta Pharm 2006; 56: 105-12.
[27] Deschamps P, Kulkarni PP, Sarkar B. X-ray structure of physiological copper(II)-bis(l-histidinato) complex. Inorg Chem 2004; 43: 3338-3340
[28] Vasconcelos MTSD, Almeida CMR. Electrochemical study of proton ionisation, copper(II) complexation and surfactant properties of piperazine-N-N'-bis[2-hydroxypropanesulfonic acid] pH buffer. Comparison with other N-substituted aminosulfonic acids pH buffers. Anal Chim Acta 1998; 369: 115-122.
[29] Bingham MJ, McArdle HJ. A comparison of copper uptake by liver plasma membrane vesicles

and uptake by isolated cultured rat hepatocytes. Hepatology 1994; 20: 1024-31.
[30] McArdle HJ, Guthrie JR, Ackland ML, Danks DM. Albumin has no role in the uptake of copper by human fibroblasts. J Inorg Biochem 1987; 31: 123-31.
[31] Bissig KD, Honer M, Zimmermann K, Summer KH, Solioz M. Whole animal copper flux assessed by positron emission tomography in the Long-Evans cinnamon rat - a feasibility study. Biometals 2005; 18: 83-88.
[32] Treichel U, Paietta E, Poralla T, Meyer zum Büschenfelde KH, Stockert RJ. Effects of cytokines on synthesis and function of the hepatic asialoglycoprotein receptor. J Cell Physiol 1994; 158: 527-34.
[33] Casey CA, McVicker BL, Donohue TM, McFarland MA, Wiegert RL, Nanji A, Liver asialoglycoprotein receptor levels correlate with severity of alcoholic liver damage in rats. J Appl Physiol 2004; 96: 76-80.
[34] Gupta S. Cell therapy to remove excess copper in Wilson's disease. Ann N Y Acad Sci 2014; 1315: 70-80.